Antimicrobial Properties of Glass Surface Functionalized with Silver-doped Terminal-alkynyl Monolayers

Muhammad Nazir Tahir, Daham Jeong, Hwanhee Kim, Jae-Hyuk Yu,[†] Eunae Cho, and Seunho Jung[*]

Department of Bioscience and Biotechnology, Bio/Molecular Informatics Center & Center for Biotechnology Research in UBITA (CBRU), Konkuk University, Seoul 143-701, Korea. [*]E-mail: shjung@konkuk.ac.kr
[†]Departments of Bacteriology and Genetics, and Molecular and Environmental Toxicology Center,
University of Wisconsin, Madison, WI, USA

Glass discs functionalized with alkynyl (GDA) terminated monolayers were prepared and incubated in AgNO$_3$ solution (GDA-Ag). The modified functional glass surfaces were characterized by X-ray photoelectron microscopy (XPS). The potential of GDA and GDA-Ag as antimicrobial surfaces was investigated. Antimicrobial efficacies of GDA against *Escherichia coli*, *Pseudomonas aeruginosa*, *Staphylococcus aureus*, *Bacillus cereus*, and *Candida albicans* was relatively low ranging from 4.67 to 17.00%. However, the GDA-Ag was very effective and its antimicrobial efficacy ranged from 99.90 to 99.99% against the same set of microbial strains except for *C. albicans* where it was 95.50%. The durability of the Ag bonded to the terminal alkynyl groups was studied by placing the GDA-Ag in PBS buffer solution (pH 7.4) for two weeks. Initially, the silver release was relatively fast, with 40.05 ppb of silver released in first 24 h followed by a very slow and constant release. To study the potential of GDA-Ag for medical applications, in vitro cytotoxicity of GDA-Ag against Human Embryonic Kidney 293 (HEK293) cell lines was studied using WST-assay. The cytotoxicity of the GDA-Ag was very low (5%) and was almost comparable to the control (blank glass disc) indicating that GDA-Ag has a promising potential for medical applications.

Key Words : Glass surface modification, Terminal alkynyls, Silver, Antimicrobial activity, Cytotoxicity

Introduction

The application of surface-modified materials is rapidly increasing in modern science and technology.[1] Different materials, *e.g.*, silicon, glass, quartz, and organic polymers are being used to manufacture functional surfaces. Among these materials, glass is more interesting because it is optically transparent at wavelengths > 320 nm and has a low intrinsic fluorescence. Moreover, it is readily available at low cost, has high mechanical stability, and is amenable to easy surface modification techniques.[2,3]

The control of microbial infections is a very important issue in the modern society. Microbes form biofilms that are attached irreversibly on a substrate or to each other.[4] Spreading of such microbial layers on different surfaces such as medical products, packing materials, and air filtration systems are problematic since the extra cellular matrix produced by the micro-organisms cause infections.[5,6] Moreover, the presence of such microbes on medical devices and other related surfaces often have serious health consequences because these surfaces provide a sanctuary for microbial communities which are tolerant to both host defense systems and antibiotic treatments.[7]

Mechanisms that facilitate the formation of microbial colonies on the surfaces are not fully understood and therefore effective prevention and therapeutic methods are still elusive to control the device-associated infections. Two strategies are commonly used to stop the microbes from infecting humans and forming microbial colonies on material surfaces. They include the application of antibiotics and impregnation of materials with biocides.[5,6] Although the application of antibiotics is simple and can slow down the growth of microbial organisms, a complete protection by this method is rare.[8] Such methods are temporary solutions, create considerable environmental pollution, and also support the development of resistant microbial strains.[6] In second method, biocides such as benzalkonium chloride,[9] iodine,[10] Irgoson,[11,12] chlorhexidine,[13] and antibiotics including dicloxacillin,[14] teicoplonin,[15] and mupirocin[16] are used to impregnate the material, which releases the antimicrobial compounds into the surroundings and kills the microbes. Most of such slow-release bioactive materials often have a limited life-span, require costly impregnation methods, and have extensive environmental concerns stemming from biofouling and biocorrosion.[8,17] Another up-coming and rapidly growing strategy is the covalent attachment of monomer or polymer layers having antimicrobial properties which can kill microbes without releasing biocides into the environment.[6] Most of these compounds have quaternary ammonium salts, biguanide groups, quaternary pyridinium salts, sulphonium salts, phosphonium salts, and other antimicrobial compounds.[5,18] By immobilizing the biocide groups, the surface will be protected against bacterial attachment for prolonged periods of time.[5]

Silver (Ag) has been known as an antimicrobial agent for centuries.[19] It is known to inhibit the attachment and growth

of microbes on any surface.[7,20,21] Silver ions (Ag^{+}) bind to sulfur-containing membranes and cytoplasmic proteins[22,23] thereby causing structural changes in nucleic acids, membranes, and cell walls that affect the DNA replication ability as well as inactivates the expression of ribosomal subunit proteins and enzymes in the bacterial strains.[24-26] Antimicrobial properties of silver have been applied in different forms such as silver-nanoparticles, nanosheets prepared from silver-modified graphene oxide,[27] and polyalkenoate cement coatings containing silver ions.[7]

It is well known that terminal alkynes can form complexes with various metal ions. Avny *et al.*,[28] found that mercury, aluminium, and silver are bound efficiently by propargylated cellulose membranes. Tahir *et al.*,[29] dialyzed pentynyl dextran against AgNO_3 solution to make an Ag complex with terminal alkyne group. A similar strategy was applied in this study to immobilize silver on modified glass surface. Our objective was to determine the feasibility of the application of silver-doped glass surface that exhibit antimicrobial and antifungal activity against a wide variety of bacteria and fungi. The results from this work have indicated that glass surface modified with terminal acetylene groups can be applied successfully to attach silver ions. Such a silver-doped modified glass surface can be used to inhibit bacterial growth on the surfaces of medical and biological devices.

Experimental

Materials. Chemicals that include 5-chloro-1-pentyne (98%), acetone (99.9%), hydrochloric acid (HCl, 37%), triethylamine (Et_3N, 99%) were purchased from Sigma-Aldrich, while 1,2-epoxy-9-decene (96%) was purchased from Tokyo Chemical Industry. Methanol (99.9%), *n*-hexane (99.9%), ethyl alcohol (99.9%), and dichloromethane (99.9%), were purchased from Duksan. AgNO_3 was purchased from Kojima Chemical Co. Ltd., Japan while glass microscope slides (76 × 26 × 1 mm) were purchased from Paul Marienfeld GmbH & Co. KG, Lauda-Königshofen, Germany and converted into round discs of 15 mm in diameter. *Escherichia coli* ATCC 8739, *Pseudomonas aeruginosa* ATCC 10145, *Bacillus cereus* ATCC 11778, *Staphylococcus aureus* ATCC 25923, and *Candida albicans* ATCC 10231 were purchased from the Korean Collection for type Culture, KR. The components of the Luria–Bertani and Sabouraud Dextrose medium used in growing and maintaining the microbial cultures were supplied by Difco Laboratories.

Water was purified using Direct-Q Millipore water purification system from SAM WOO S&T CO., Ltd. Korea. The 1,2-epoxy-9-decene was further purified by column chromatography (EtOAc/Et_2O 3:1), while other chemicals were used without further purification or any other treatment.
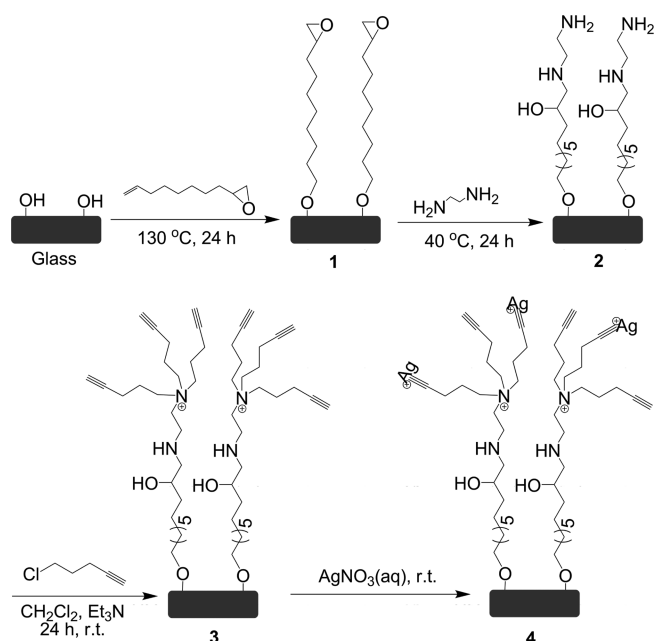
X-ray Photoelectron Spectroscopic (XPS) spectra were recorded by using a Sigma Probe (ThermoVG, UK) photoelectron spectrometer. High-resolution spectra were obtained using monochromatic *Al-Kα* X-ray radiation at 15 kV and 100 W and an analyzer pass energy of 50 eV (1.0 eV step size) for wide-scan and 20 eV (0.1 eV step size) for

narrow-scan. All high-resolution spectra were corrected with a linear background before fitting.

Modification of Glass Discs. Glass disc modification was carried out as described in a previous publication.[30] Glass discs were cleaned with acetone, *n*-hexane, methanol, and ethanol followed by sonication for 5 min per solvent and etched for 30 min in a freshly prepared solution of hydrochloric acid (37%) and ethanol (1:1 v/v). After etching, the discs were rinsed with ultrapure water and methanol for 5 min per solvent, and dried under nitrogen stream. Immediately after cleaning, the glass discs were transferred into a glass reaction cell specially designed for this purpose. Glass discs were coated with 1,2-epoxy-9-decene under a nitrogen atmosphere before tightly closing the reaction cell. To remove the traces of oxygen and moisture that might enter the reaction cell during glass discs coating, it was dipped into liquid nitrogen to freeze the coated 1,2-epoxy-9-decene on glass (while under nitrogen atmosphere) and allowed to liquefy again at room temperature under vacuum. This freeze-thaw cycle was repeated three times. Finally, the reaction cell was filled with nitrogen, dipped into silicon oil bath and heated at 130 °C for 24 h while under slight nitrogen pressure. The modified glass discs (**1** in Scheme 1) were removed from the reaction cell and washed thoroughly with deionized water, *n*-hexane, and acetone followed by sonication for 5 min per solvent and dried under nitrogen stream.

Subsequently, the glass discs (**1**) were transferred to degassed fresh 1,2-ethylenediamine. The reaction was carried out at 40 °C for 24 h followed by washing and drying, as described in the previous step.

Terminal alkynyl group was attached onto the amine-terminated glass discs (**2**) *via* a reaction with 5-chloro-1-pentyne (0.55 g, 5.4 mM, 0.5 mL) in dry dichloromethane (8 mL) and Et_3N (1 mL) at room temperature for 24 h followed by cleaning and drying steps (all quantities are given for a

Scheme 1. Functionalization of the glass disc surface.

set of 3 glass discs).

Glass discs functionalized with alkynyl-terminated mono-layer (GDA, **3**) were incubated in aqueous AgNO$_3$ solution (2.5%) for 48 h at room temperature. AgNO$_3$ solution was replaced with fresh solution after 24 h. Ag doped glass discs (GDA-Ag, **4**) were washed thoroughly with deionized water to remove unbound Ag salt and dried under nitrogen. The amount of silver bound to the terminal alkynyl group was determined from elemental composition and narrow scan XPS Ag$_{3d}$ spectra. The experiment was repeated three times and an average of three measurements was obtained.

Determination of Antimicrobial Activity of Modified Glass Surface (4). The round glass discs (1.3 cm in diameter) functionalized with alkynyl terminated mono layer (GDA, **3**) and treated with AgNO$_3$ (GDA-Ag, **4**) after sterilization with 70% ethanol were incubated with standardized cell suspension of microbes (0.3 mL, 1×10^7 CFU/mL) in wells of 24-well nonclon tissue culture plates for 24 h at 37 °C (bacteria, *E. coli*, *P. aeruginosa*, *B. cereus*, *S. aureus*), or 30 °C (yeast, *C. albicans*) with 150 rpm in an incubator. Along with the GDA-Ag, samples with GDA, and blank glass were also prepared in parallel. After 24 h, the microbial culture was transferred to a new plate and serially diluted with medium and enumerated using CFU counts. The antimicrobial efficacy of GDA (**3**) and GDA-Ag (**4**) was calculated according to the Eq. (1):

$$\text{Antimicrobial efficacy (\%)} = \frac{V_c - V_t}{V_c} \times 100 \qquad (1)$$

Where V_c and V_t represent the number of viable bacterial colonies of the blank glass and test modified glass (GDA, GDA-Ag), respectively.

Silver Ion Release. The *in vitro* release of silver ions from GDA-Ag (**4**, 1.3 cm in diameter) was analyzed in 0.3 mL of 20 mM phosphate buffered saline (PBS, pH = 7.4). The samples were incubated at 37 °C and 150 rpm in an incubator. The samples were collected from the incubation medium after 6, 12, 24, 120, and 360 h and the concentration of Ag ions released in the medium was determined by inductively coupled plasma mass spectrometry (ICP-MS) (ELAN 6100, Perking-Elmer CIEX, Canada).

Cell Culture. The Human Embryonic Kidney 293 (HEK293) cell lines were purchased from a Korean Cell Line Bank (Seoul, Korea). The cells were maintained in Eagle's minimum essential medium (MEM, WelGENE Inc., Daegu, Korea) supplemented with 10% heat-inactivated fetal bovine serum (FBS, WelGENE Inc., Daegu, Korea), 1% antibiotics (100 U/mL penicillin and 100 μg/mL strepto-mycin) at 37 °C in a humidified incubator at 5% CO$_2$.

Cytotoxicity Assay. WST-1 (4-[3-{4-iodophenyl}-2-{4-nitrophenyl}-2*H*-5-tetrazolio]-1.3-benzene disulfonate) test was employed for cytotoxicity assessment.[31] Cells were grown on the blank glass (control), GDA (**3**), and GDA-Ag (**4**) in 24-well plates at a concentration of 3×10^4 cells/well for 24 h. The amount of cell proliferation was determined using WST-1 assay after 24 h incubation.

Results and Discussion

Modification of Glass Surface. Surface modification of glass discs was initiated with the epoxide terminated mono-layer (Scheme 1) as described in the experimental section [30]. Wide-scan X-ray photoelectron spectroscpy (XPS) spectrum (Figure 1(a)) displayed the signal for C$_{1s}$ (285.00 eV), O$_{1s}$ (533.0 eV) and Si$_{2p}$ (103.0 eV). The narrow-scan C$_{1s}$ region of XPS displayed a signal at 285.0 eV corresponding to C-C bonds resulting from alkyl chain and a signal at 286.81 eV (Figure 1(b)) corresponding to C-O bonds.[30] The ratio of C-O/C-C is 0.41, which is in agreement with the theoretical value of 0.43. These results indicate that high quality ep-oxide monolayers on the glass surface were obtained. The thickness of the formed epoxide layer, calculated using Eq. (2), was 1.12 nm, which is slightly higher than the length of 1,2-epoxy-9-decene (1.11 nm, as calculated with Chem3D). This confirmed that the process employed in this study resulted in the formation of a monolayer.

$$I_{si} = I_{si}^{\infty} \exp\left(\frac{-d}{\lambda_{si,c} \cos\theta}\right) \qquad (2)$$

Variables, I_{si} (the absolute silicon peak intensity), I_{si}^{∞} (the absolute silicon peak intensity of unmodified glass), d (the thickness of the adsorbed layer), $\lambda_{si,c}$ (the attenuation length of Si$_{2p}$ electrons in the hydrocarbon layer), and θ (the
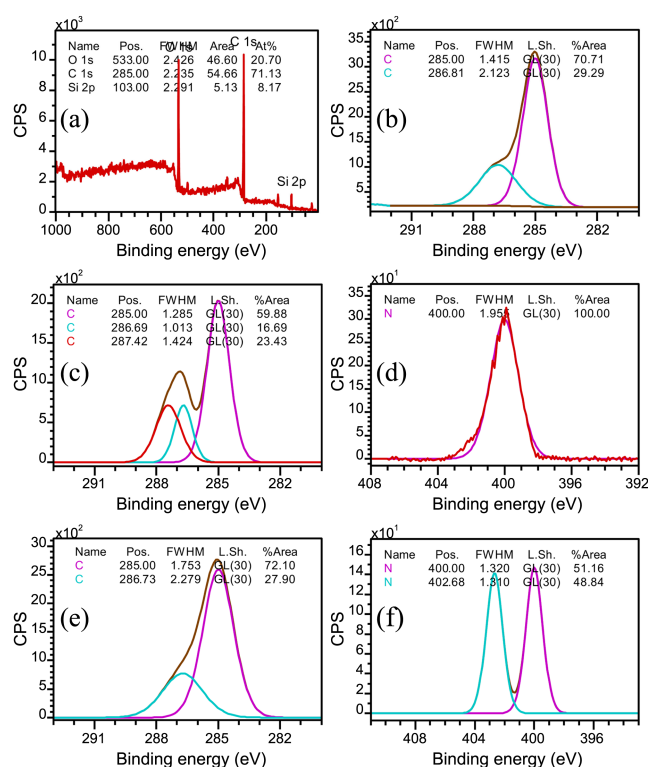

Figure 1. XPS spectra of different steps of glass discs function-alization: Wide-scan XPS spectrum of epoxide terminated mono-layer (a, **1**), narrow-scan C$_{1s}$ spectrum for epoxide terminated mono-layer (b, **1**), narrow-scan C$_{1s}$ (c, **2**), and N$_{1s}$ (d, **2**) for amine terminated mono-layer, and narrow-scan C$_{1s}$ (e, **3**), and N$_{1s}$ (f, **3**) for alkynyl terminated mono-layer.

42   *Bull. Korean Chem. Soc.* **2014**, Vol. 35, No. 1

Muhammad Nazir Tahir et al.

electron takeoff angle), were calculated from XPS data as described in a previous publication.[32]

The epoxide-terminated glass surface was subsequently converted into an amine terminated surface *via* a reaction with ethylenediamine. In XPS spectra, three signals, corresponding to C-C (285.0 eV), C-O (286.69 eV), and C-N (287.42 eV) appeared (Figure 1(c)). The similarity between the measured (0.67) and theoretical (0.71) value for C-X/C-C (C-X denotes combined value of C-O + C-N bond linkages) indicate the successful reaction of amine with epoxide and corresponds to 94% attachment of 1,2-ethylenediamine onto the epoxide-terminated surface. In addition, the appearance of a signal of organic nitrogen at 400 eV from the resultant monolayer (Figure 1(d)) also indicates the successful attachment of 1,2-ethylenediamine onto the epoxide-terminated glass surface.

Terminal alkyne groups were attached to the amine-terminated surfaces *via* a reaction of 5-chloro-1-pentyne with the amine group already attached to the surface using the method described in experimental part. XPS narrow-scan C_{1s} spectrum (Figure 1(e)) displayed a signal at 285 eV that corresponds to C-C bond linkages while a broad signal at 286.73 eV corresponds to the overlapped signal for C-N and C-O linkages. Theoretical value of (C-C)/(C-O + C-N) (2.38, calculated according to the structure shown in Scheme 1, **3**) is in agreement with the experimental value of 2.58 and corresponds to 92% conversion of amine terminated monolayer (**2**) into alkynyl terminated monolayer (**3**). The appearance of an additional signals in N_{1s} region at 402.68 eV along with the usual nitrogen signal at 400 eV (Figure 1(f)) indicate that the terminal amine was converted into quaternary ammonium cation.[30] Relative ratio of two N_{1s} signals calculated from its narrow-scan XPS spectrum (Figure 1(f)) was 0.95 (theoretical value 1.0) and show that 95% of the terminal amine (-NH$_2$) was converted into its quaternary cation ($\equiv$N$^+$-). All these results confirm the successful reaction of pentynyl chloride with the amine terminated monolayer.

For the formation of a silver complex with the terminal alkynyl group, glass disc functionalized with alkynyl groups (GDA, **3**) was incubated in 2.5% AgNO$_3$(aq) solution for 48 h (24+24) and characterized by XPS. Wide-scan XPS spectrum of glass disc functionalized with alkynyl terminated monolayer (GDA, **3**) after treatment with Ag (GDA-Ag, **4**) show Ag_{3d} signal at 368 eV along with other signals for O, C N, and Si (Figure 2(a)). Atomic percent of Ag is 0.26% which corresponds to 0.006:1 to Ag:CCH bonds (calculated according to the structure shown in Scheme 1, **4**). Moreover, the appearance of a couple of signals at 368.20 eV ($Ag_{3d3/2}$) and 374.23 eV ($3d_{5/2}$) in XPS narrow scan Ag_{3d} spectrum (Figure 2(b)) also confirm the presence of Ag. The 6.0 eV splitting of the 3d doublet signal for Ag (Figure 2(b)) indicate that some of the Ag was converted into metallic Ag.[27,33] As Ag can be oxidized easily in the presence of oxygen, it is possible that part of the Ag on the glass surface was oxidized. However, the signal corresponding to lattice oxygen O^{-2} from Ag$_2$O was not observed. Narrow-scan C_{1s}
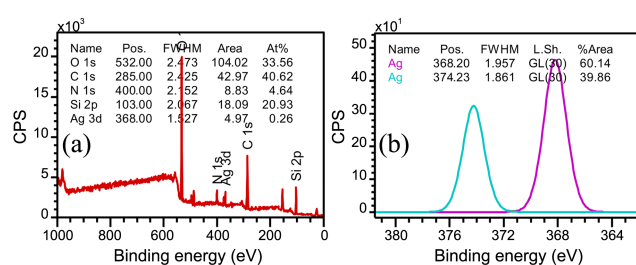

Figure 2. XPS wide-scan (a) and narrow-scan Ag_{3d} (b) spectrum of alkynyl terminated mono layer after treatment with AgNO$_3$ solution (GDA-Ag, **4**).

XPS spectra of GDA-Ag (**4**, not shown here, see SI) show almost the same proportion of (C-C)/(C-O + C-N) (2.43) as recorded for this surface before incubation with AgNO$_3$ solution (Figure 1(e)), indicating the absence of degradation or any other structural change in the monolayers grafted on the glass surface.

Antimicrobial Activity of Functional Glass Surface. The antimicrobial activity of GDA (**3**) and GDA-Ag (**4**) was assessed by applying viable cell counting methods against Gram-negative (*E. coli*, *P aeruginosa*), Gram-positive (*S. aureus*, *B. cereus*) bacteria and Fungi (*C. albicans*). *E. coli*, *B. Cereus* are widespread intestinal parasites of mammals, and *P. aeruginosa*, and *S. aureus* infect the mammals. *C. albicans* is the most common fungal pathogen that causes mucosal and systemic infection. The activity of GDA (**3**) and GDA-Ag (**4**) in inhibiting the growth of these test microbes are show in Figure 3. The antimicrobial efficacies of the GDA (**3**) against *E. coli*, *P aeruginosa*, *S. aureus*, *B. cereus*, and *C. albicans* were respectively 17.0%, 8.4%, 4.67%, 5.4%, and 17.0%. These results indicate that GDA (**3**) was not much effective against the microbes tested in this study. On the other hand, when GDA-Ag (**4**) was used as the antimicrobial surface against the same group of microbes, it was very effective and the antimicrobial efficacies were: *E. coli* 99.99%, *P. aeruginosa* 99.94%, *S. aureus* 99.99%, *B.*
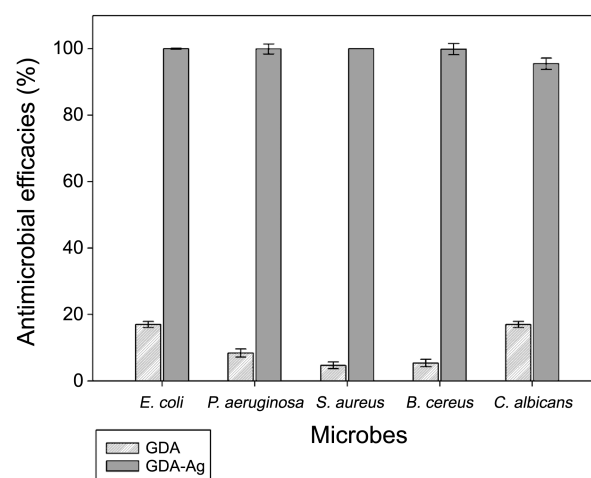

Figure 3. Antimicrobial activity of GDA (**3**) and GDA-Ag (**4**) against different microbes assessed using viable cell counting method. All results are expressed as an average of three experiments.

cereus 99.90%, and *C. albicans* 95.50%. Comparative analysis of these results (summarized in Figure 3) and the structure of GDA (**3**) and GDA-Ag (**4**) indicate that along with the quaternary ammonium ion (present in both structures **3** and **4**), the terminal Ag ion influences the antimicrobial activity.

Silver Ion Release from the Functional Glass Surface (4). Release of the bound silver ions into the solution is directly linked to the stability and antimicrobial efficacy of the modified surface. During this study, Ag ion release form the GDA-Ag (**4**) was investigated in a PBS buffer solution (Figure 4) and the amount of the Ag ions released into the buffer solution was measured by inductively coupled plasma-mass spectrometry (ICP-MS). The terminal acetylene group of GDA (**3**) forms a complex with Ag ions, which is mainly responsible for the antimicrobial effect of modified glass surface against the various microbes (Figure 3). Ag ion release studies (Figure 4) indicate that the silver release was fast for the first 24 h followed by a slow but consistent release for almost the next two weeks. Although, the silver release for the first 24 h was relatively faster, the total Ag ions released during this period was only 40.05 ppb (Figure 4). Nevertheless, a 0.1 ppb of Ag ions concentration is adequate to inhibit the growth of the microbes tested in this study. Lee *et al.*, [34] studied the activity of Ag ions against *S. aureus* and *E. coli* by adding 150 μL (10^8 CFU mL^{-1}) of 400 ppb Ag solution and reported that the antimicrobial activity was only 50%. However, in this study, although the Ag release was very low (Figure 4) its antimicrobial activity was very high (Figure 3 and 5). The growth inhibiting effect of GDA-Ag (**4**) was tested against *E. coli*, *P. aeruginosa*, *S. aureus*, *B. cereus*, and *C. albicans* with agar plating (Figure 5). Blank cleaned glass discs were used as control in parallel. As shown in Figure 5, there was no growth around the discs where GDA-Ag (**4**) was used while there was a rapid growth in the control. Since the GDA-Ag releases Ag ion very slowly (Figure 4) into the surrounding medium, its inhibiting effect around the disc also depends upon the relative growth rate of the microbes. The growth rate of the *C. albicans* is relatively slower than the other Gram-negative and Gram-positive bacteria used in this study. Therefore, the clear zone (Figure 5(e)) is relatively larger than that of the other micro-
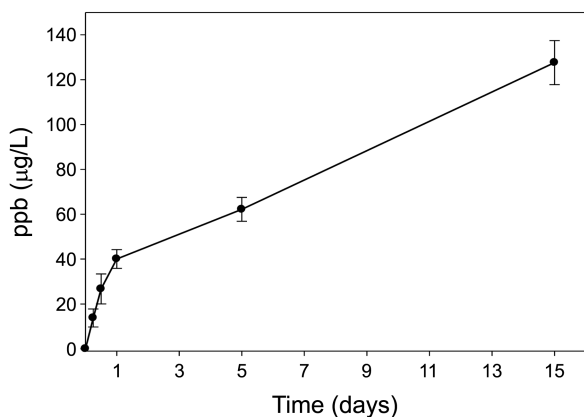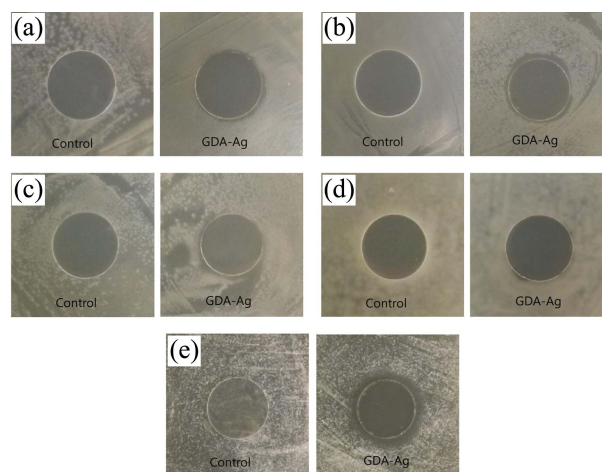

Figure 5. Comparison of the antimicrobial efficacy of blank glass (control) and GDA-Ag (**4**) glass for *E. coli* (a), *P. aeruginosa* (b), *S. aureus* (c), *B. cereus* (d), and *C. albicans* (e) with agar plating.

bes. On the other hand, *B. cereus* has the property of very fast-growing colonies. Therefore, almost no clear zone was observed in this case (Figure 5(d)). Moreover, *C. albicans* is different in nature from the other bacterial strains used in this study and grow better under anaerobic conditions. Therefore, its colonies were also observed under the covered part of the glass (Figure 5(e)) in the control samples (blank glass) but it was not observed in case of GDA-Ag due to its strong bacterial inhibiting properties. These results confirm the strong antimicrobial abilities of the GDA-Ag (**4**) surface. Also these results indicate that strong antimicrobial activity of the GDA-Ag is not only due to the Ag released into the medium but the Ag attached to the terminal alkynyl groups (see **4** in Scheme 1) is also involved in inhibiting the bacterial growth.

***In vitro* Cytotoxicity Assay.** *In vitro* cell cytotoxicity studies evaluate the biocompatibility potential of the materials for medical applications. In this study, we conducted the biocompatibility assessment of GDA-Ag (**4**) to assure bio-safety using the WST-assay as described in the experimental section. The cytotoxicity results, summarized in Figure 6, indicate the cytotoxicity of control (blank glass) and that of
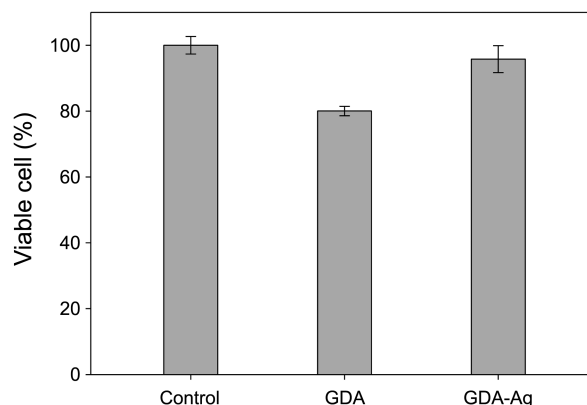

Figure 4. Silver ion release curve of GDA-Ag (**4**) in PBS (pH 7.4) (n = 3).

Figure 6. Cytotoxicity of control (blank clean glass), GDA (**3**), and GDA-Ag (**4**) against HEK 293 cells (n = 3).

GDA (**3**) and GDA-Ag (**4**) against HEK 293 cells. There was almost no difference between the control and GDA-Ag. Even though Ag can be released from GDA-Ag (Figure 4), the cytotoxicity of GDA (**3**) is 19.8% and still less than the acceptable for medical device.[35] Therefore, GDA-Ag (**4**) is a material that has a promising potential for medical applications.

Conclusions

The results of this study indicates that the glass surface functionalized with alkynyl terminated monolayer (GDA, **3**) having quaternary ammonium cation and with Ag ions incubated with alkynyl monolayer (GDA-Ag, **4**) have antimicrobial properties. GDA-Ag (**4**) was very effective against a variety of microbial strains. Also GDA-Ag (**4**) was very effective in inhibiting the growth of the microbes. The modified glass surface was very stable and only a very small amount of Ag was released in to the buffer solution over the period of two weeks. Although the released Ag can kill the bacteria, our results indicate that the amount released was inadequate and the bound silver (GDA-Ag, **4**) was mainly responsible for killing a variety of microbes. Finally, the *in vitro* cytotoxicity studies of DGA-Ag against HEK293 cells indicated that GDA-Ag was quite safe for medical applications due to its low cytotoxicity, which is much lower than the cytotoxicity levels acceptable in medical devices.

References

1. Manz, A.; Becker, H. *Microsystem Technology in Chemistry and life Science*; Springer: Heidelberg, 1998.
2. Henry, C. S. *Methods in Molecular Biology*; Totowa: Humana Press, 2006.
3. Kuzmin, A.; Poloukhtine, A.; Wolfert, M. A.; Popik, V. V. *Bioconjugate Chem.* **2010**, *21*, 2076.
4. Donlan, R. M.; Costerton, J. W. *Clin. Microbiol. Rev.* **2002**, *15*, 167.
5. Khaled, M.; Abu-Sharkh, B.; Khalil, A.; Manda, A.; Amr, E. *Open Nanomed. J.* **2008**, *1*, 1.
6. Siedenbiedel, F.; Tiller, J. C. *Polymers* **2012**, *4*, 46.
7. Coughlan, A.; Boyd, D.; Douglas, C.; Towler, M. *J. Mater. Sci. Mater. Med.* **2008**, *19*, 3555.
8. Donlan, R. M. *Emerg Infect Dis.* **2001**, *7*, 277.
9. Jansen, B.; Kirstinsson, K. G.; Jansen, S.; Peters, G.; Pulverer, G. *J. Antimicrob. Chemother.* **1992**, *30*, 135.
10. Tebbs, S. E.; Elliott, T. S. J. *J. Antimicrob. Chemother.* **1993**, *31*, 261.
11. Kingston, D.; Birnie, E. D. C.; Martin, J.; Pearce, P. C.; Manek, S.; Quinn, C. M. *J. Hosp. Infect.* **1992**, *20*, 257.
12. Kingston, D.; Seal, D. V.; Hill, I. D. *J. Hyg.* **1986**, *96*, 185.
13. Castillo, J. A.; Pinazo, A.; Carilla, J.; Infante, M. R.; Alsina, M. A.; Haro, I.; Clapés, P. *Langmuir* **2004**, *20*, 3379.
14. Sherertz, R. J.; Forman, D. M.; Solomon, D. D. *Antimicrob. Agents Chemother.* **1989**, *33*, 1174.
15. Jansen, B.; Jansen, S.; Peters, G.; Pulverer, G. *J. Hosp. Infect.* **1992**, *22*, 93.
16. Hill, R. L. R.; Fisher, A. P.; Ware, R. J.; Wilson, S.; Casewell, M. W. *J. Hosp. Infect.* **1990**, *15*, 311.
17. Schofield, W. C. E.; Badyal, J. P. S. *Appl. Mater. Interfaces* **2009**, *1*, 2763.
18. Huang, J.; Koepsel, R. R.; Murata, H.; Wu, W.; Lee, S. B.; Kowalewski, T.; Russell, A. J.; Matyjaszewski, K. *Langmuir* **2008**, *24*, 6785.
19. Wichner, N. M.; Beckers, J.; Rothenberg, G.; Koller, H. *J. Mater. Chem.* **2010**, *20*, 3840.
20. Sampath, L. A.; Chowdhury, N.; Caraos, L.; Modak, S. M. *J. Hosp. Infect.* **1995**, *30*, 201.
21. Cook, G.; Costerton, J. W.; Darouiche, R. O. *Int. J. Antimicrob. Agents* **2000**, *13*, 169.
22. Bragg, P. D.; Rainnie, D. J. *Can. J. Microbiol.* **1974**, *20*, 883.
23. McDonnell, G.; Russell, A. D. *Clin. Microbiol. Rev.* **1999**, *12*, 147.
24. Maneerung, T.; Tokura, S.; Rujiravanit, R. *Carbohydr. Polym.* **2008**, *72*, 43.
25. Feng, Q. L.; Wu, J.; Chen, G. Q.; Cui, F. Z.; Kim, T. N.; Kim, J. O. *J. Biomed. Mater. Res. A* **2000**, *52*, 662.
26. Yamanaka, M.; Hara, K.; Kudo, J. *Appl. Environ. Microbiol.* **2005**, *71*, 7589.
27. Ma, J.; Zhang, J.; Xiong, Z.; Yong, Y.; Zhao, X. S. *J. Mater. Chem.* **2011**, *21*, 3350.
28. Avny, Y.; Rahman, R.; Zilkha, A. *J. Macromol. Sci. Chem.* **1972**, *6*, 1427.
29. Tahir, M. N.; Bork, C.; Risberg, A.; Horst, J. C.; Komoß, C.; Vollmer, A.; Mischnick, P. *Macromol. Chem. Phys.* **2010**, *211*, 1648.
30. Nguyen, A. T.; Baggerman, J.; Paulusse, J. M. J.; van Rijn, C. J. M.; Zuilhof, H. *Langmuir* **2011**, *27*, 2587.
31. Hilmi, F.; Gertsch, J.; Bremner, P.; Valovic, S.; Heinrich, M.; Sticher, O.; Heilmann, J. *Bioorg. Med. Chem.* **2003**, *11*, 3659.
32. ter Maat, J.; Regeling, R.; Yang, M.; Mullings, M. N.; Bent, S. F.; Zuilhof, H. *Langmuir* **2009**, *25*, 11592.
33. Gunawan, C.; Teoh, W. Y.; Marquis, C. P.; Lifia, J.; Amal, R. *Small* **2009**, *5*, 341.
34. Lee, J. S.; Murphy, W. L. *Adv. Mater.* **2013**, *25*, 1173.
35. Marques, A. P.; Reis, R. L.; Hunt, J. A. *Biomaterials* **2002**, *23*, 1471.